Nanocrystallite Regions of Guar Gum Filled PU/PAN Composites Before and After Biodegradation Using WAXS

H. Kumar,[1] Siddaramaiah,[2] R. Somashekar,[3] S. S. Mahesh,[3] A. Manjunath[3]

[1]*Fiber Science and Apparel Design, Cornell University, Ithaca, New York 14853*
[2]*Department of Polymer Science and Technology, Sri Jayachamarajendra College of Engineering, Mysore 570 006, India*
[3]*Department of Studies in Physics, University of Mysore, Mysore 570 006, India*

Received 18 August 2006; accepted 7 March 2007
DOI 10.1002/app.27332
Published online 25 February 2008 in Wiley InterScience (www.interscience.wiley.com).

ABSTRACT: Polyurethane/polyacrylonitrile semi-interpenetrating polymer network containing varying weight percent of guar gum were prepared. The resulting composites were subjected to biodegradation with the help of specific fungi *Aspergillus niger*. The composite before and after biodegradation were subjected to wide angle X-ray scattering studies. The nanocrystallite regions, area, and size are determined from X-ray data using three different asymmetric column length functions. A comparison of these parameters does explain the nature of biodegradation at microlevel. © 2008 Wiley Periodicals, Inc. J Appl Polym Sci 108: 2762–2771, 2008

Key words: biodegradable; interpenetrating networks; nanolayers; polyurethanes; WAXS

INTRODUCTION

Ever since the development of polymeric material cellophane, from cellulose, exploitation of naturally occurring polymers like polysaccharides, proteins, polyesters, etc., is in progress. Among the naturally occurring polymers, starch has been extensively used along with synthetic polymers as biodegradable polymer composites or blends.[1–8] There were efforts to use chitosan-based polymers as biodegradable polymer.[9–13] The use of wood and plant-derived fillers by the thermoplastic industry has been growing.[14,15] Extensive literature survey revealed that semi-interpenetrating polymer networks (SIPN) derived from castor oil-based polyurethane (PU) and derivatives of natural polymers, such as nitrocellulose,[16] nitrokonjak glucomannan,[17] and benzyl konjak glucomannan[18,19] were studied. Studies on guar gum (GG)-filled polyurethane/polyacrylonitrile (PU/PAN) SIPNs have not received much attention. GG is a high molecular mass hydrocolloidal polysaccharide belonging to the family *Leguminosae*, composed of galactan and mannan units combined through glycoside linkages that may be described chemically as galactomannan.

It is essential to know the degradation behavior of composites and its effect on the mechanical and structural properties. Many researchers studied the behaviour of degraded polymer composites and found that the degradation reactions occur predominantly in the amorphous region and are controlled by the diffusion of oxygen in this region,[20] while chain scission occurs in the amorphous phase of the polymer.[21] There are several publications on composite matrix structure investigation by DSC and microscopy.[22–25] However, only a few attempts have been made to investigate the nanocrystallite regions of these polymers through the use of X-ray scattering.[26–29] The characterization of polymer composites by wide angle X-ray scattering (WAXS) for single-walled carbon nanotubes (SWCN) filled PAN was reported by Sreekumar et al.[28] They noticed the better interaction between PAN and SWCN, that lead to enhanced tensile modulus. Similarly, Seferisi et al.[29] studied carbon fiber reinforced polyethylene terephthalate (PET) and polyether ether ketone (PEEK) for degree of crystallinity and orientation of carbon fibers. There are no reported studies on GG-filled PU/PAN SIPN. In this work, the naturally occurring GG in different weight percent namely, 5, 10, and 30% by weight were filled into PU/PAN (50/50) SIPN by *in situ* polymerization. The degradation by fungi *Aspergillus niger* has been reported. The GG-filled PU/PAN IPN composites before and after degradation were characterized by WAXS studies.

Correspondence to: Siddaramaiah (siddaramaiah@yahoo.com).

Journal of Applied Polymer Science, Vol. 108, 2762–2771 (2008)

EXPERIMENTAL

Materials

Polyethylene glycol-400 (PEG) (M/s. Ranbaxy Laboratories, India), benzoyl peroxide (Aldrich, St. Louis, MO), and 4,4′-diphenyl methane diisocyanate (MDI) (Merck, Whitehouse Station, NJ) were used as such. Acrylonitrile (SD Fine Chem., Boisor, India) monomer was freed from stabilizer prior to use. GG (Shree Vinayaka Corporation, Jodhpur, India) was dried under vacuum before it is being used. The stains of *Aspergillus niger* was supplied by Green guard Biotech, Bangalore.

Preparation of samples

A mole of PEG-400 was made to react with 1.5 moles of 4,4′-diphenyl methane diisocyanate (MDI) in the presence of 0.05 wt % of new catalyst to obtain PU prepolymer.[30] The 50% by weight of acrylonitrile monomer with 0.5% of benzoyl peroxide and 5, 10 and 30 wt % of GG were added into the pre PU mixture. The reaction mixture was stirred thoroughly at room temperature for 30 min and then poured into a clean glass mould sprayed with releasing agent. The mould was kept in a closed chamber at room temperature for 12 h for PU polymerization. The temperature of the mould was then slowly raised to 80°C and allowed for 12 h to polymerize acrylonitrile by free radical sequential polymerization.[31,32] The resulting opaque golden yellow to light brown PU/PAN/GG composites were cooled slowly and taken out of the mould.

Biodegradation studies

About 1 g PU/PAN/GG composites containing different weight ratios of GG was taken in Erlenmeyer flask with 50 mL of potato-dextrose broth (PDB). This mixture was sterilized in an autoclave at 120°C for 40 min. The sterilized composite-PDB mixtures were inoculated with 2 mL of *Aspergillus niger* (AN) spore suspension. The flasks were placed on a rotary shaker at room temperature (25°C) in dark for 30 days. The samples were sterilized, dried, and characterized by WAXS.

Wide angle X-ray scattering

X-ray powder pattern of GG-filled PU/PAN (50/50) SIPN were recorded on Philips PW 1140 diffractometer of Bragg-Branto Geometry (fine focus setting) with germanium filtered monochromatic radiation of Cu K_α (λ = 0.1542 nm) for 2θ range 3–60° in steps of 0.03°,by employing a curved position sensitive detector (CPSD) in the transmission mode. These patterns were indexed using TREOR procedure.

Microstructural parameters crystal size ($<N>$) and lattice strain (g in %) are usually determined by employing Fourier method reported elsewhere.[33–35] The intensity of a profile in the direction joining the origin to the center of the reflection can be expanded in terms of Fourier cosine series;

$$I(s) = \sum_{n=-\infty}^{\infty} A(n)\cos\{2\pi nd(s - s_0)\} \quad (1)$$

where, the coefficients of the harmonics $A(n)$ are functions of the size of the crystallite and the disorder of the lattice. Here, s is sin (θ)/(λ), s_0 is the value of s at peak of a profile, n is the harmonic order of the coefficient, and d is the lattice spacing. The Fourier coefficients can be expressed as;

$$A(n) = A_s(n)A_d(n) \quad (2)$$

For a paracrystalline material, $A_d(n)$ can be obtained, with Gaussian strain distribution;[35,36]

$$A_d(n) = \exp(-2\pi^2\, m^2 n g^2) \quad (3)$$

Here, ''m'' is the order of the reflection and g = ($\Delta d/d$) is the lattice strain. Normally one also defines mean square strain $<\varepsilon^2>$ which is given by g^2/n. This mean square strain is dependent on n, whereas g is not.[37,38] For a probability distribution of column lengths $P(i)$, we have;

$$A_s(n) = 1 - \frac{nd}{D} - \frac{d}{D}\left[\int_0^n iP(n)di - n\int_0^n P(i)di\right] \quad (4)$$

where $D = <N>d_{hkl}$ is the crystallite size and ''i'' is the number of unit cells in a column. In the presence of two orders of reflections from the same set of Bragg planes, Warren and Averbach[33] have given a method of obtaining the crystal size ($<N>$) and lattice strain (g in %). But in polymer it is very rare to find multiple reflections. So, to obtain the finer details of microstructure, we approximate the size profiles by simple analytical function for $P(i)$ by retaining only the asymmetric functions. Another advantage of this method is that the distribution function is not the same along different directions. Whereas, a single crystal size distribution function is used for the whole pattern fitting, which we feel, may be inadequate to describe polymer diffraction patterns.[37–39] Here, it is emphasized that the Fourier method of profile analysis (single order method used here) is quite reliable one according to the recent survey and results of Round Robin test conducted by IUCr.[40] In fact for refinement, we have also included the effect of background by introducing a parameter[41] [see for details regarding the effect of background on the microcrystalline parameters].

The exponential distribution

It is assumed that there are no columns containing fewer than p unit cells and those with more decay exponentially. Thus, we have;[42,43]

$$A_s(n) = \begin{cases} A(0)(1 - n/ < N >); & \text{if } n \le p \\ A(0)\{\exp[-\alpha(n-p)]\}/(\alpha N); & \text{if } n \ge p \end{cases} \quad (5)$$

Here, ''α'' is the width of the distribution function, ''i'' is the number of unit cells in a column, ''n'' is the harmonic number, ''p'' is the smallest number of unit cells in a column, and $<N>$ is the number of unit cells counted in a direction perpendicular to the (hkl) Bragg plane.

The Lognormal distribution

The Lognormal distribution function is;[37,43]

$$A_s(n) = \frac{m^3 \exp[(9/4)(2^{1/2}\sigma)^2}{3} \times \operatorname{erfc}\left[\frac{\log(|n|/m)}{2^{1/2}\sigma} - \frac{3}{2}2^{1/2}\sigma\right] - \frac{m^2 \exp(2^{1/2}\sigma)^2}{2}|n|\operatorname{erfc}\left[\frac{\log(|n|/m)}{2^{1/2}\sigma} - 2^{1/2}\sigma\right] + \frac{|n|^3}{6}\operatorname{erfc}\left[\frac{\log(|n|/m)}{2^{1/2}\sigma}\right] \quad (6)$$

where σ is the variance and m is the median of the distribution function.

Reinhold distribution

With the exponential distribution function, $P(i)$ rises discontinuously at p, from zero to its maximum value. In contrast, the Reinhold function allows a continuous change;[43]

$$A_s(n) = \begin{cases} A(0)(1 - n/ < N >); & \text{if } n \le p \\ [A(0)(n - p + 2/\beta)/N]\{\exp[-\beta(n-p)]\}; & \text{if } n \ge p \end{cases} \quad (7)$$

$$\beta = 2/(N - P) \quad (8)$$

where β is the width of the distribution which has been varied to fit the experimental results with p as the smallest number of unit cells in a column,[37,42] N is the number of unit cells counted in a direction perpendicular to the (hkl) Bragg plane; d, the spacing of the (hkl) planes; λ, the wavelength of X-rays used; i, the number of unit cell in a column; n, the harmonic number; and D_s is the surface weighted nanocrystal size ($<N>d_{hkl}$).

All the distribution functions were put to test in order to find out the most suitable crystal size distribution function for the profile analysis of the X-ray diffraction. The procedure adopted for the computation of the parameters is as follows. Initial values of g and $<N>$ were obtained using Nandi et al.[44] Substituting these values in the equations mentioned earlier in the text, gives the corresponding values for the width of distribution. These are only rough estimates, so the refinement procedure must be sufficiently robust to start with such values. Here, we compute;

$$\Delta^2 = [I_{cal} - (I_{exp} + BG)]^2/npt \quad (9)$$

where BG parameter represents the error in the background estimation, npt is the number of data points in a profile, I_{cal} is the intensity calculated using eqs. (1)–(9), and I_{exp} is the experimentally measured intensity. The values of Δ were divided by half the maximum value of intensity so that it is expressed relative to the mean value of intensities, and then minimized. For refinement against intensities, the multidimensional minimization algorithm of the SIMPLEX method was used.[41]

RESULTS AND DISCUSSION

We have reported[45] the mechanical behavior of GG-filled PU/PAN composites before and after biodegradation. Tensile behavior was found to be in the order; $0 < 5 < 10 > 30$ before biodegradation, whereas after degradation it was found to decrease drastically with the increase in GG.

WAXS before biodegradation

The X-ray intensity profiles for selected GG-filled PU/PAN composites are shown in Figure 1. The reflection maxima with the corresponding spacing (d) are listed in Table I. As shown in Figure 1, all the samples showed two convoluted diffuse scattering reflection in the 2θ range of 3–60°; the first reflection is broad with very high intensity in the 2θ range 15.26°–21.46°, and second reflection (shoulder) is again broad but weak in 2θ range 20°–43.75°. D'Orazio et al. noticed the reflections in these regions for ether based elastomeric PU and such results suggested an amorphous structure.[46–48] Microcrystalline parameters like nanocrystal size ($<N>$) and lattice strain (g in %) for GG-filled PU/PAN IPNs were calculated using three different asymmetric distribution functions and the results are given in Table I. To ascertain the most suitable asymmetric distribution, fitness test was made using line profile simulation from the peak of the reflection

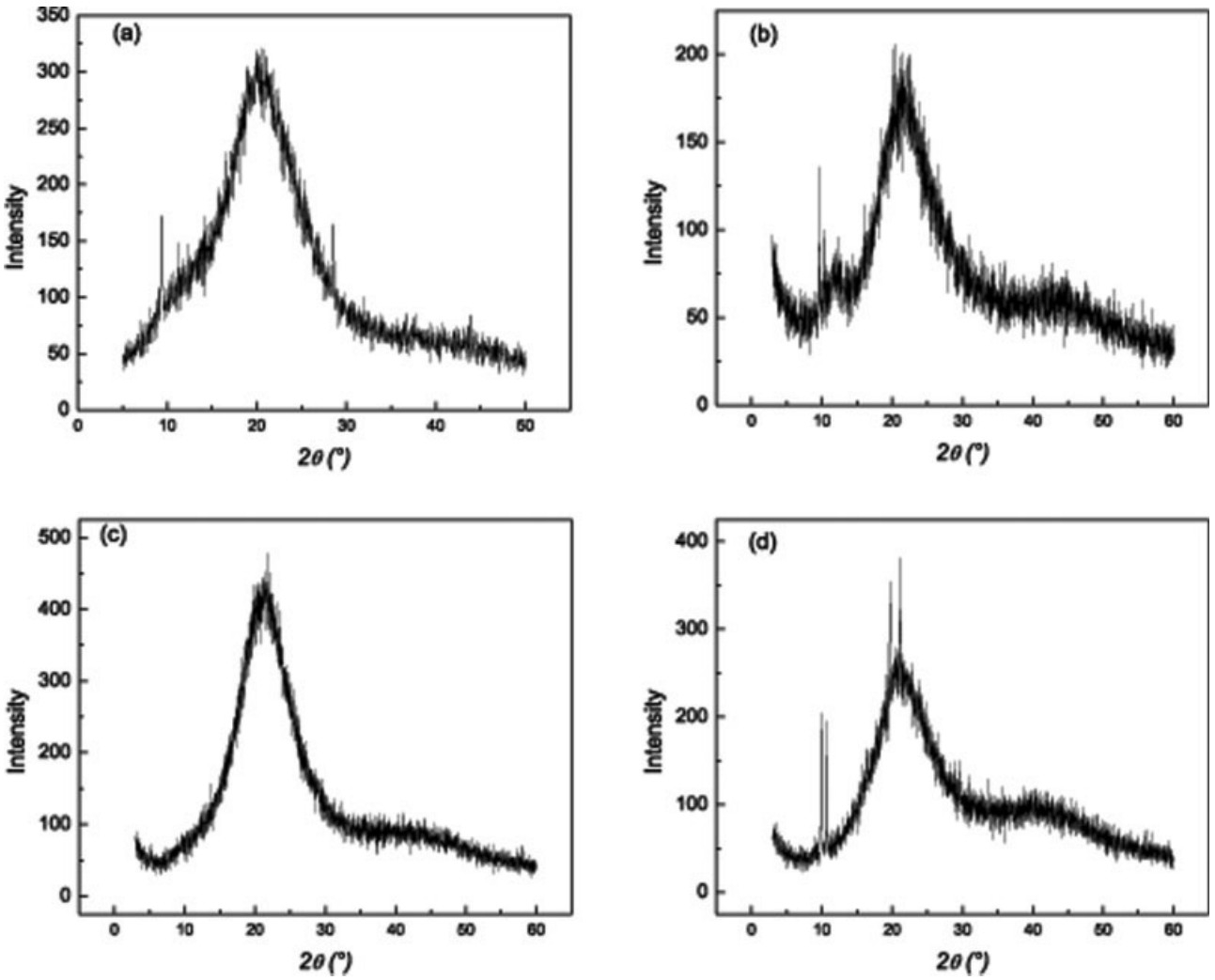

Figure 1 X-ray profile of (a) 0%, (b) 5%, (c) 10%, and (d) 30% GG-filled PU/PAN composites.

to the base line of it. Experimental and simulated X-ray profiles for GG-filled PU/PAN composites calculated by using all the distribution functions and specimen profiles for 10% and 30% GG-filled PU/PAN IPNs for both main and shoulder peaks are shown in Figure 2(a–d), respectively. It is evident from these figures that there is a good agreement between experimental and theoretically calculated X-ray data for exponential distribution function. In all the cases the goodness of the fit was less than 15%. From Table I, it is also evident that the exponential distribution has less standard deviation (δ) compared to other distribution functions and hence, we have preferred the corresponding results for further interpretation.

TABLE I
Microstructural Parameters Obtained from X-ray Pattern for PU/PAN (50/50) Samples with Different Amount of GG by Employing Exponential (Exp), Reinhold (Rein), and Lognormal (Log) Distribution Functions Before Biodegradation

		Crystallite area in nm			<N>		δ (%)			g (%)			α		
% of PS	2θ (°)	Exp	Rein	Log	Exp	Rein	Exp	Rein	Log	Exp	Rein	Log	Exp	Rein	*d* in nm
0	15.26	0.951	0.8556	0.79.18	1.75	1.68	0.06	0.06	0.06	0.4	0.5	0.5	3.16	3.90	0.581
	20.0				2.11	2.10	0.03	0.03	0.04	0.5	0.5	0.5	1.44	2.13	0.443
5	21.46	0.7771	0.7729	0.6573	2.57	2.55	0.02	0.03	0.04	0.5	0.5	0.5	1.24	1.80	0.414
	43.75				3.53	3.54	0.03	0.03	0.04	0.5	0.5	0.5	1.78	2.98	0.207
10	21.2	0.4881	0.4881	0.3928	2.71	2.71	0.03	0.03	0.04	0.7	0.7	0.5	2.97	4.39	0.419
	37.42				1.79	1.79	0.06	0.06	0.08	0.7	0.7	0.5	8.35	4.80	0.24
30	21.19	0.5737	0.5737	0.4745	2.71	2.71	0.03	0.03	0.04	0.7	0.5	0.7	3.73	5.45	0.419
	40.0				2.24	2.24	0.03	0.03	0.04	0.6	0.5	0.5	3.95	7.51	0.225

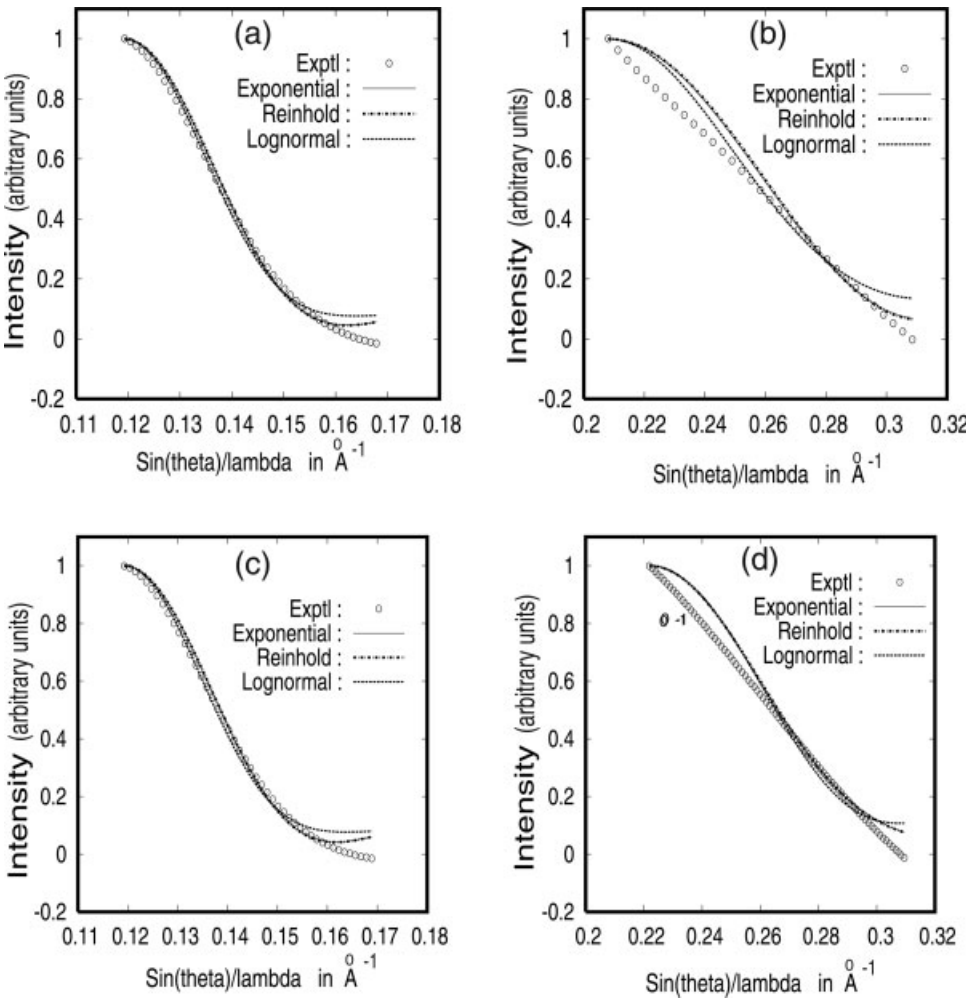

Figure 2 Experimental and simulated X-ray profiles for (a) 0% (b) 5%, (c) 10%, and (d) 30% GG-filled PU/PAN composites before biodegredation using Exponential, Reinhold, and Lognormal distribution functions.

The surface weighted nanocrystal size (D_s) obtained by exponential distribution as a function of weight percent of GG is shown in Figure 3. It was observed that the incorporation of GG into PU/PAN matrix was found to increase the surface weighted crystal size of the main peak, whereas the shoulder peak D_s value reduced upto 10% GG-filled systems. Further increase in GG content was found to increase the value of D_s. The variation in D_s is related to the values of crystal size [$<N>$] and lattice strain (g), and indicate the variation in the behavior of GG filled PU/PAN IPNs due to change in structure and morphology with compositions.

The nanocrystallite area obtained from all the distribution functions for all the samples were compared with the corresponding tensile strength and is shown in Figure 4(a–c). From the figures it is evident that these two are reciprocal to each other.

Incorporation of GG into PU/PAN matrix is found to decrease the interplanar distance (d) as evident from Figure 5. But, an increase in GG content is

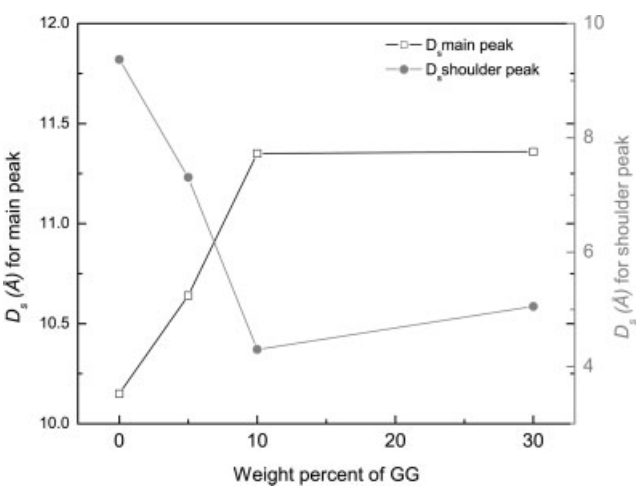

Figure 3 Surface weighted crystal size (D_s) as a function of GG for main and shoulder peaks obtained from exponential distribution function for PU/PAN/GG.

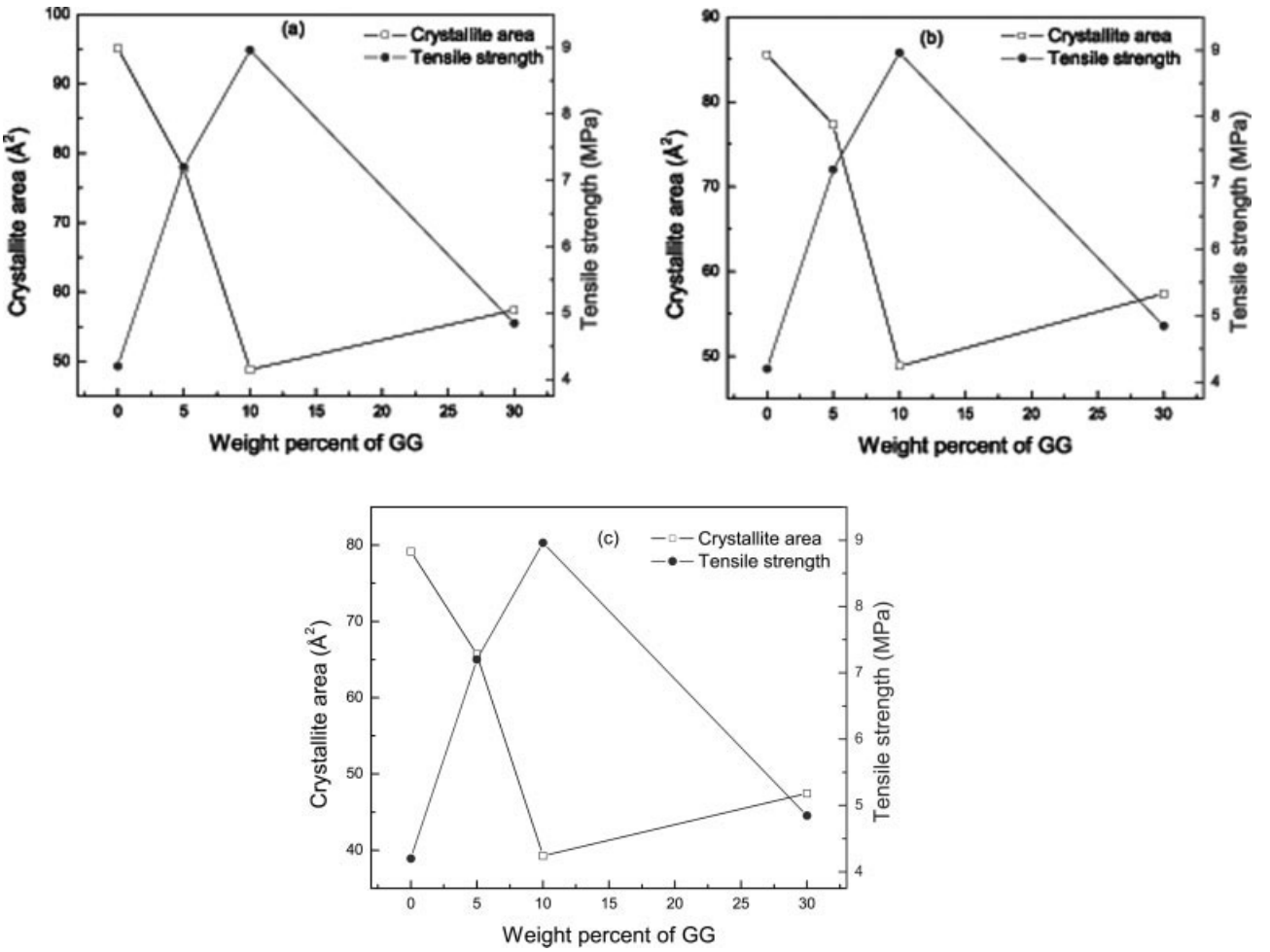

Figure 4 Tensile strength and crystallite area obtained by (a) Exponential, (b) Reinhold, and (c) Lognormal as a function of weight percent of GG of the composite.

found to increase the interplanar distance corresponding to both the 2θ values. However, interplanar distance of main peak was found to be lesser than corresponding value of shoulder peak, but the variation is same. This implies that there is change in the structure of the composite system with increase in GG content.

WAXS after biodegradation

The X-ray profiles of selected GG filled PU/PAN IPNs after biodegradation are shown in Figure 6. Table II contains the reflection maxima with corresponding spacing along with the other microstructural parameters generated using three asymmetric distribution functions.

The scattering reflections of all the specimens showed two broad reflections of variable intensity, the first major peak in the 2θ range of 21°–21.55° and the second shoulder reflection in 2θ range of 40°–48.08°. Shift in the 2θ values of both the peaks were

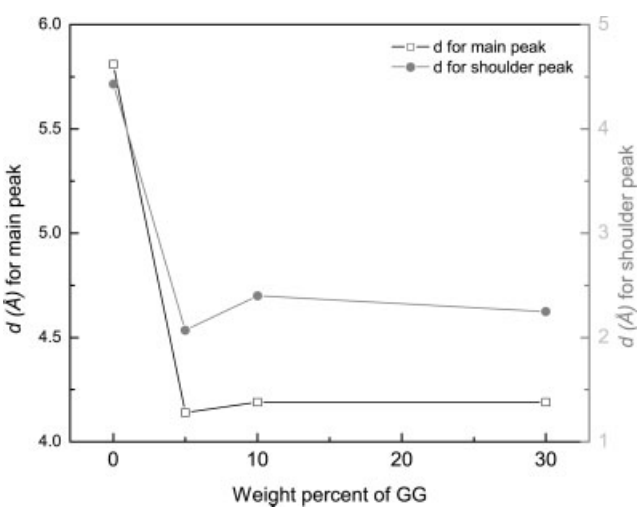

Figure 5 Change in interplanar distance as a function of weight percent of GG for the composite before biodegradation.

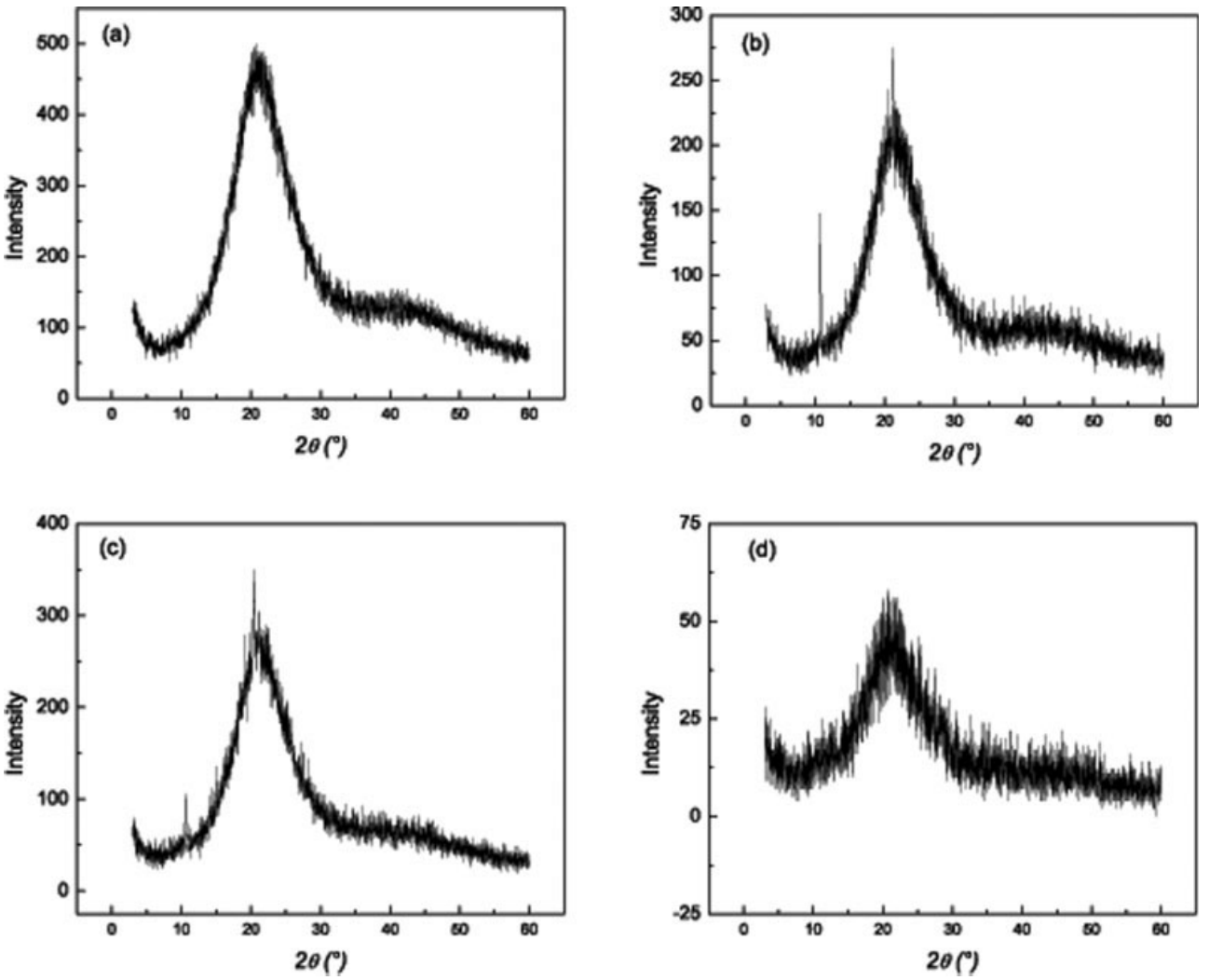

Figure 6 X-ray profiles of (a) 0%, (b) 5%, (c) 10%, and (d) 30% GG-filled PU/PAN composites after biodegradation.

observed as compared to 2θ values that were there before biodegradation. A notable change is observed in the intensity of reflections. The increase in GG content was found to decrease the intensity of first reflection, though the change is not systematic. The decrease in intensity of broad peak indicates the change in structure of material caused by biodegradation.

Experimental and simulated X-ray profiles were obtained for PU/PAN/GG composites using all the distribution functions and representative X-ray profiles for 5 and 30% GG-filled PU/PAN systems for

TABLE II
Microstructural Parameters for PU/PAN (50/50) Samples with Different Amount of GG After Biodegradation by Employing Exponential (Exp), Reinhold (Rein), and Lognormal (Log) Distribution Functions

		Crystallite area in nm			<N>		δ (%)			g (%)			α		
% of PS	2θ (°)	Exp	Rein	Log	Exp	Rein	Exp	Rein	Log	Exp	Rein	Log	Exp	Rein	*d* in nm
0	21.55	0.4756	0.4761	0.4073	2.70	2.70	0.03	0.03	0.04	1	0.4	0.4	1.47	2.24	0.412
	40.00				1.90	1.90	0.02	0.03	0.03	0.5	1.3	1.5	7.50	1.00	0.225
5	21.53	0.9204	0.9225	0.7805	2.79	2.8	0.04	0.03	0.05	0.5	0.5	0.5	4.34	3.89	0.413
	42.78				3.78	3.78	0.01	0.02	0.03	0.5	0.5	0.5	7.45	3.78	0.211
10	21.32	0.5275	0.525	0.4596	2.69	2.69	0.03	0.03	0.05	0.5	0.3	0.3	2.31	3.32	0.417
	40.00				2.09	2.08	0.03	0.04	0.05	0.5	0.3	0.3	1.20	1.72	0.225
30	21.00	1.4831	1.4831	1.2202	2.20	2.20	0.02	0.02	0.05	0.5	0.5	0.5	4.77	9.13	0.423
	48.08				8.42	8.42	0.02	0.02	0.03	0.1	0.1	0.1	9.16	9.83	0.189

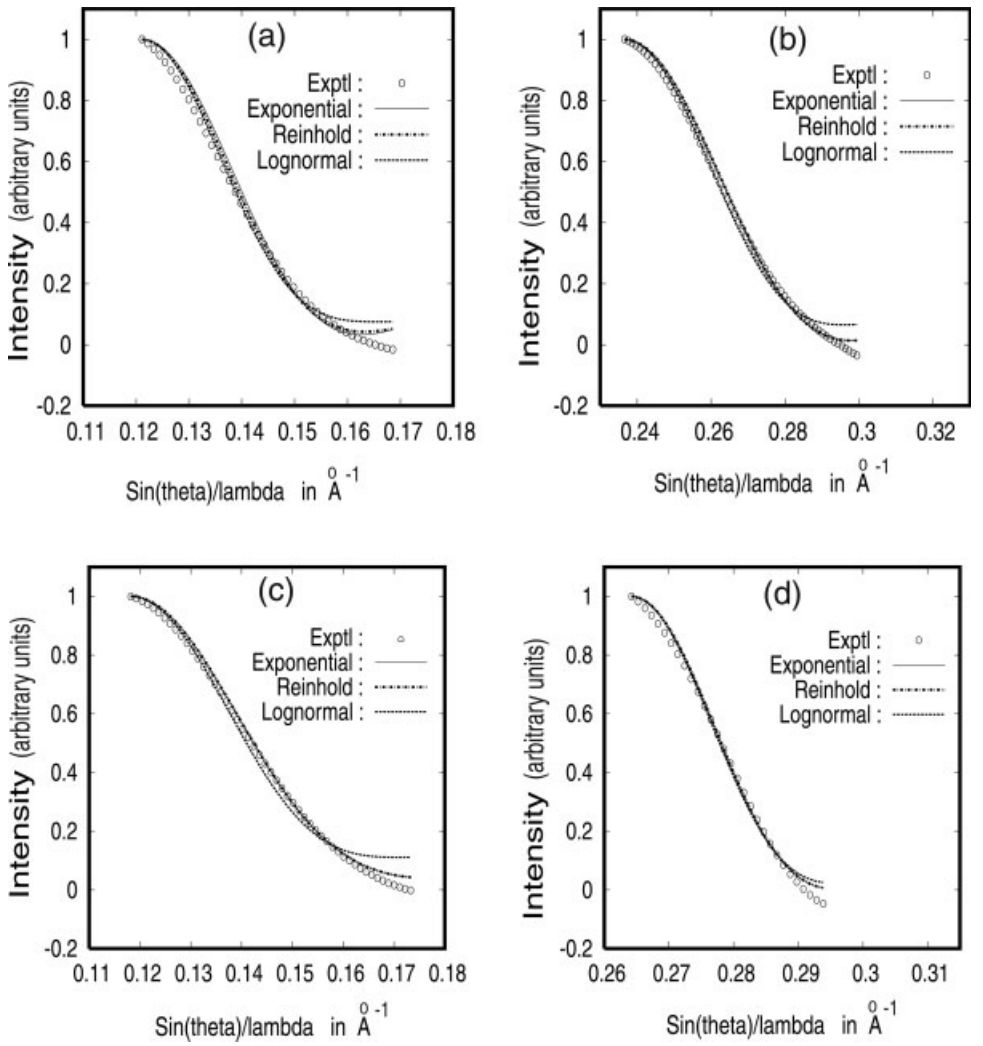

Figure 7 Experimental and simulated line profiles for (a,b) 5% and (c,d) for 30% GG-filled PU/PAN composites after biodegradation using Exponential, Reinhold, and Lognormal distribution functions.

both main and shoulder peaks are shown in Figure 7(a–d). It is evident from these figures that there is a good agreement between experimental and theoretically calculated X-ray data for exponential distribution function. From Table II, it is also evident that the exponential distribution has less standard deviation (δ) compared to other distribution functions and hence, we have preferred the corresponding results for further interpretation.

The variation of surface weighted nanocrystallite size (D_s) with weight percent of GG is shown in Figure 8 for main and shoulder peak. The surface weighted crystallite size D_s was found to decrease for main peak whereas for shoulder peak is increased with the increase in GG content. This phenomenon is quite reversal for specimens before biodegradation. The crystallite area after biodegradation (Table II) is found to increase with increase in GG content whereas before biodegradation, it was found to decrease (Table I) with increase in GG. This result

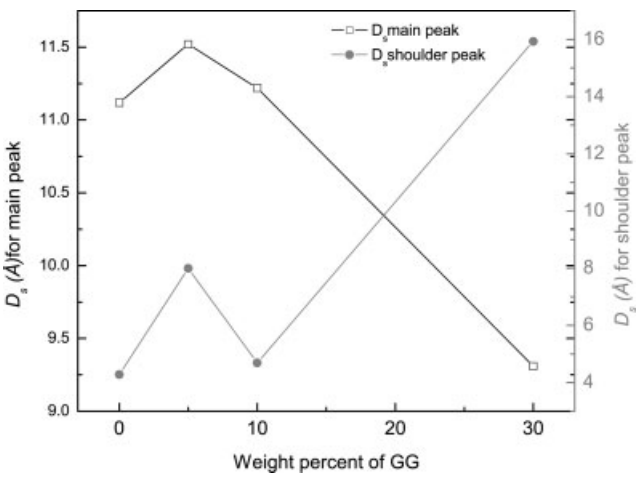

Figure 8 Surface weighted crystal size for main and shoulder peak obtained from Exponential distribution function after biodegradation.

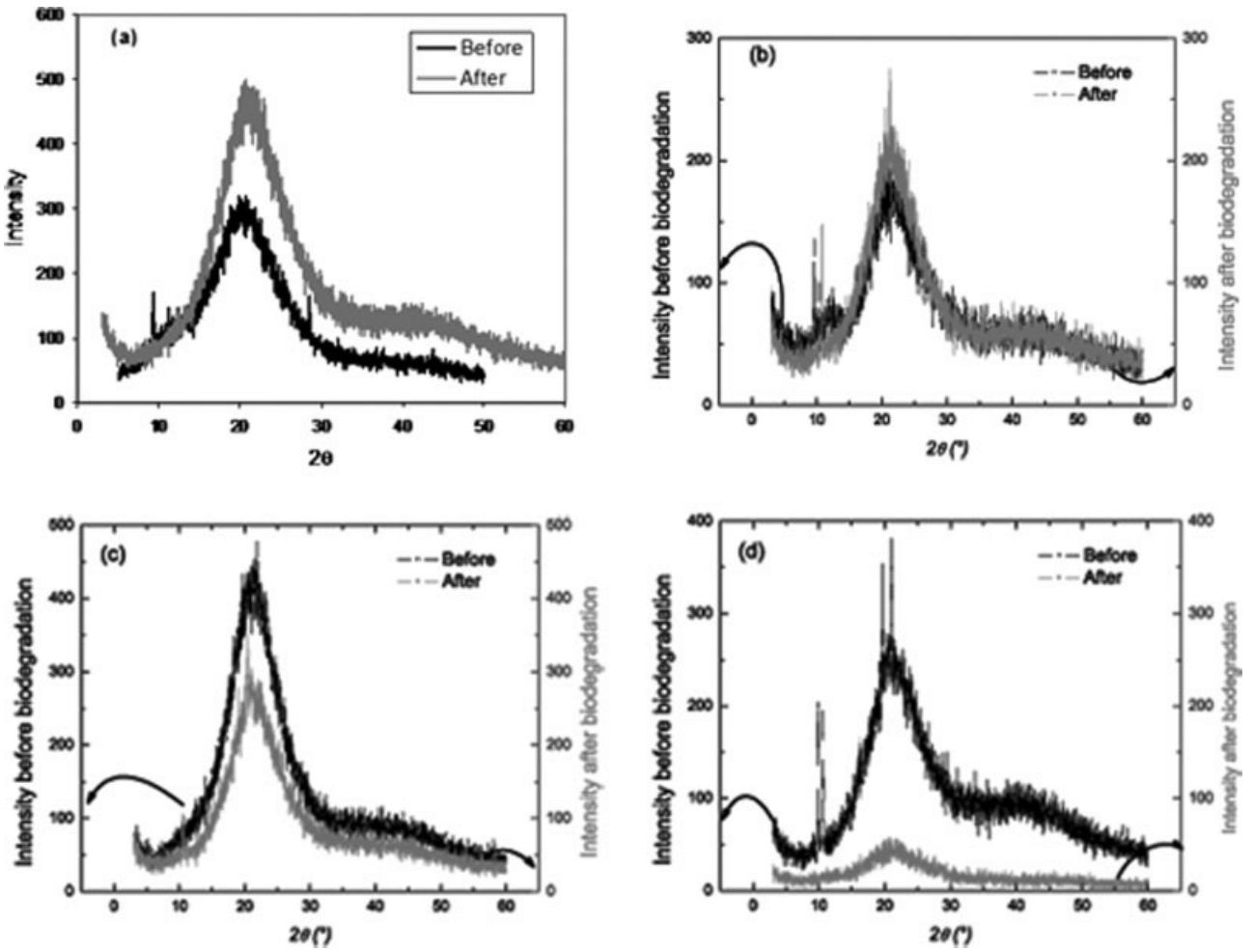

Figure 9 X-ray profiles of (a) 0%, (b) 5%, (c) 10%, and (d) 30% GG-filled PU/PAN composites before and after biodegradation in *Aspergillus niger.*

suggests that there is a change in structural behavior of material because of biodegradation.

It is evident from Figure 9 that there is decrease in intensity of peaks, with the increase in weight percent of GG. It was observed that the increase in GG was found to increase the biodegradation and that the amorphous component of the composite system undergoes biodegradation.[49–53] In our earlier communication, we have found that the fractional free volume measured by positron annihilation lifetime spectroscopy (PALS) decreased after biodegradation.[53] This implies the degradation of easily vulnerable soft and amorphous segment. This supports the molecular rearrangement due to degradation of amorphous component of composites in the presence of *Aspergillus niger*.

The change in nanocrystallite area of the composite is very interesting. The crystallite area of PU/PAN matrix was found to decrease after biodegradation. For GG-filled PU/PAN, the nanocrystallite area was found to be large for biodegraded specimens compared to specimens before biodegradation. This could be due to degradation of amorphous component and realignment of molecules after biodegradation. The increase in nanocrystallite area also

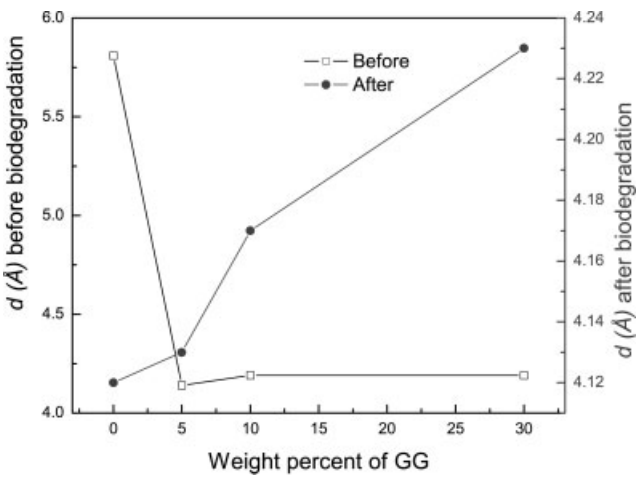

Figure 10 Variation of interplanar distance after biodegradation as a function of weight percent of GG of composite.

supports the decrease in fractional free volume observed for the same system.[53] This change will also affect the rate of biodegradation. It was observed that the rate biodegradation for 30% GG filled composite is less compared to other composites. This could be due to increase in inter and intramolecular hydrogen bonding between the components of composite.

From Figure 10, it is observed that the interplanar distance is found to increase drastically with the increase in GG content after biodegradation, whereas the trend is quite reverse before biodegradation. This, once again confirms the change in structure of composite system. Biodegradation of polymer composites probably destabilizes the crystalline network defects and brings about the narrowing of reflections. As a result, the calculated nanocrystallite size decreases and interplanar distance increases.[54]

CONCLUSIONS

Nanocrystallite size of PU/PAN matrix is reduced after biodegradation but, the addition of GG, exhibits different X ray pattern. The nanocrystallite area increases for PU/PAN/GG after biodegradation and the percentage of increase in nanocrystallite area increases with the increase in GG content of the samples. This may hamper biodegradation process since the materials will have relatively large number of inter and intra weak hydrogen bonds in the polymer network. The process of biodegradation of GG-filled IPN gets slower because of increase in nanocrystallite area.

Authors wish to thank Dr. T. N. Guru Row and Ms. Geetha S. Kini of Department of Solid State and Structural Chemistry, Indian Institute of Science, Bangalore, for XRD.

References

1. Cao, X.; Zhang, L. Biomacromolecules 2005, 6, 671.
2. Goheen, S.; Wool, R. P. J Appl Polym Sci 1991, 42, 2691.
3. Vaidya, U. R.; Bhattacharya, M. J Appl Polym Sci 1991, 52, 617.
4. Shogren, R. L.; Thompson, A. R.; Felker, F. C.; Harry-O'kuru, R. E.; Gordon, S. H.; Greene, R. V.; Gould, J. M. J Appl Polym Sci 1992, 44, 1971.
5. Koenig, M. F.; Huang, S. J. Polymer 1995, 36, 1877.
6. Bikiaris, D.; Aburto, J.; Alric, I.; Borredon, E.; Botev, M.; Betchev, C.; Panayiotou, C. J Appl Polym Sci 1999, 71, 1089.
7. Vikman, M.; Hulleman, S. H. D.; Van Der Zee, M.; Myllorinen, P.; Feil, H. J Appl Polym Sci 1999, 74, 2594.
8. Wool, R. P.; Raghavan, D.; Wagner, G. C.; Billieux, S. J Appl Polym Sci 2000, 77, 1643.
9. Gong, P.; Zhang, L. J Appl Polym Sci 1998, 68, 1313.
10. Gong, P.; Zhang, L. J Appl Polym Sci 1998, 68, 1321.
11. Hu, S.-G.; Jou, C.-H.; Yang, M.-C. J Appl Polym Sci 2002, 86, 2977.
12. Wu, C.-S.; Lai, S. M.; Liao, H. T. M. J Appl Polym Sci 2002, 85, 2905.
13. Wu, C.-S. Polymer 2005, 46, 147.
14. Smith, P. M. US Woodfiber-polymer Composite Decking Market, Proceedings of Progress in Wood Fiber–Plastic Composites; Sixth International Conference on Woodfiber-Plastic composites, Forest Product Society, Madison, WI, 2002.
15. Stark, N. M.; Matuana, L. M. Polym Degrad Stab 2004, 86, 1.
16. Zhang, L.; Zhou, Q. J Polym Sci Part B: Polym Phys 1999, 37, 1623.
17. Gao, S.; Zhang, L. Macromolecules 2001, 34, 2202.
18. Lu, Y.; Zhang, L. Polymer 2002, 43, 3979.
19. Lu, Y.; Zhang, L. Polymer 2003, 44, 6689.
20. Wypych, G. Handbook of Material Weathering, 2nd ed.; Chem Tec: Ontario, 1995.
21. Hamid, S. H.; Amin, M. B. J Appl Polym Sci 1995, 55, 1385.
22. Blundell, D. J.; Osborn, B. N. Polymer, 1983, 24, 953.
23. Lee, Y.; Porter, R. S. Polym Eng Sci 1986, 26, 9.
24. Velisaris, C. N.; Seferis, J. C. Polym Eng Sci 1986, 26, 22.
25. Seferis, J. C.; Allstrom, C.; Dillman, S. Proc SPE ANTEC 1987, 87, 1467.
26. Hsu, T. C.; Geil, P. H. J Mater Sci 1989, 24, 4.
27. Nelson, K. M.; Seferis, J. C.; Zachmann, H. G. J Appl Polym Sci 1991, 42, 1289.
28. Sreekumar, T. V.; Liu, T.; Min, B. G.; Guo, H.; Kumar, S.; Huuge, R. H.; Smalley, R. E. Adv Mater 2004, 16, 58.
29. Seferis, J. C.; Moore, D. R.; Zachmann, H. G. Pure Appl Chem 1993, 65, 1581.
30. Kumar, H.; Siddaramaiah. Indian Pat. Application 354/CHE/2006 (2006).
31. Siddaramaiah; Mallu, P.; Somashekar, R. J Appl Polym Sci 1998, 68, 1739.
32. Sperling, L. H. Macromol Rev 1977, 12, 141.
33. Warren, B. E.; Averbach, B. L. J Appl Phys 1950, 21, 595.
34. Warren, B. E. Acta Cryst 1955, 8, 483.
35. Warren, B. E. X-ray Diffraction; Addison-Wesley: New York, 1969.
36. Hall, I. H.; Somashekar, R. J Appl Cryst 1991, 24, 1051.
37. Ribarik, R.; Ungar, T.; Gubicza, J. J Appl Cryst 2001, 34, 669.
38. Popa, N. C.; Balzar, D. J Appl Cryst 2002, 35, 338.
39. Scardi, P.; Leoni, M. Acta Cryst A 2001, 57, 604.
40. Balzar. D. IUCr Newsletter 2002, 28, 14.
41. Somashekar, R.; Hall, I. H.; Carr, P. D. J Appl Cryst 1989, 22, 363.
42. Somashekar, R.; Somashekarappa, H. S. J Appl Cryst 1997, 30, 147.
43. Kumar, H.; Siddaramaiah; Somashekar, R.; Mahesh, S. S.; Abhishek, S.; Guru Row, T. N.; Geetha S. K. J Appl Polym Sci 2006, 99, 177.
44. Nandi, R. K.; Kho, H. K.; Schlosberg, W.; Wissler, G.; Cohen, J. B.; Crist, B., Jr. J Appl Cryst 1984, 17, 22.
45. Kumar, H.; Radha, J. C.; Ranganathaiah, C.; Siddaramaiah. Euro polym J, unpublished result.
46. D'Orazio, L.; Gentile, G.; Mancarella, C.; Martuscelli. E.; Massa, V. Polym Test 2001, 20, 227.
47. Quay, J. R.; Sun, Z.; Blackwell, J.; Briber, R. M.; Thomas, E. L. Polymer 1990, 31, 1003.
48. Hwang, K. K. S.; Wu, G.; Lin, S. B.; Cooper, S. J Polym Sci Polym Chem Ed 1984, 22, 1677.
49. Kumar, H.; Ranganathaiah, C.; Siddaramaiah. Polym Test, unpublished result.
50. Griffin, J. L. In Proceedings of Symposium on Degradable Plastics; Society of Plastic Industry: Washington DC, 1987; p 44
51. Gould, J. M.; Gordon, S. H.; Dexter, L. B.; Swanson, C. L. In Agricultural and Synthetic Polymers —Biodegradability and Utilization; Glass, J. E.; Swift, G., Ed.; American Chemical Society: Washington DC, 1990; ACS Symposium Series 433, Chapter 7, p 65.
52. Chiellini, E.; Solaro, R.; Corti, A.; Picci, G.; Leporini, C.; Pera, A.; Vallini, G.; Donaggio, P. Chim Ind 1991, 8/9, 656.
53. Bikiaris, D.; Panayiotou, C. J Appl Polym Sci 1998, 70, 1503.
54. Binias, D.; Boryniec, S.; Binias, W. Fibres Textiles in East Euro 2005, 13, 137.